

Structural Analysis of Simulated Fission-Produced Noble Metal Alloys and Their Superconductivities

Yong Joon Park,^{*} Jong-Gyu Lee,^{*} Kwang Yong Jee, Young Duk Huh,[‡] and Won Ho Kim

Nuclear Chemistry Research Team, Korea Atomic Energy Research Institute, P.O. Box 105, Yusong, Taejeon 305-600, Korea

[†]Research Center, Oriental Chemical Industries, Incheon 402-040, Korea

[‡]Department of Chemistry, Dankook University, Seoul 140-714, Korea

Received July 25, 2000

Ternary (Mo-Ru-Pd) and binary (Mo-Ru, Mo-Pd) alloys have been prepared using an Ar arc melting furnace. Mo and the noble metals, Ru and Pd, are the constituents of metallic insoluble residues, which were found in the early days of post-irradiation studies on uranium oxide fuels. In the present study, the structure of the alloys was evaluated using a powder X-ray diffractometer. Unit cell parameters were determined by least squares refinements of powder X-ray diffraction data. Scanning electron microscopic analyses of the surface of the alloys indicated that surface morphology was dependent on the crystallographic structure as well as its composition. Measurements of the magnetic susceptibility of the alloys showed evidence of superconducting transition from 3 to 9.2 K. Among the ternary and binary alloys, the σ -phase showed the highest superconducting transition temperature, ~ 9.2 K.

Introduction

White metallic inclusions composed of the noble metals (ruthenium, rhodium and palladium), technetium and molybdenum are formed in nuclear fuel during irradiation.¹ Structural information as well as data on the physical, chemical and thermodynamic properties of these metallic inclusions are of great importance due to their insolubility in UO_2 . This knowledge can be critical in the case of an accident involving a nuclear power reactor or in the case of dissolution in the recovery and separation processing of spent nuclear fuel.

Since molybdenum, ruthenium and palladium are fission products with the major yields, these three metals can be representative of the fission-produced metallic inclusions. Investigations on the constitution and thermodynamics of the ternary system have been carried out in wide temperature ranges by many researchers.²⁻⁴ Phase studies on the pseudo-ternary system (Mo-Ru-Rh_{0.5}Pd_{0.5}) at 1700 °C performed by Kleykamp *et al.* revealed the existence of extended four mono-phases (hcp ϵ , fcc α , bcc β , tetragonal σ), five two-phases ($\beta + \epsilon$, $\beta + \sigma$, $\sigma + \epsilon$, $\alpha + \epsilon$ and $\alpha + \text{L}$) and one three-phase ($\beta + \epsilon + \sigma$).^{2,13} However, the hexagonal close-packed (hcp) ϵ phase identified in the insoluble residue derived from simulated nuclear fuel after dissolution with HNO_3 appears in the corresponding ternary sections in a broad concentration range.⁵⁻⁷

One of the hexagonal close packed ϵ phases identified in the insoluble residue by single crystal diffraction measurements was Mo-Tc-Ru-Pd (36 : 20 : 34 : 10), and its lattice parameters (S.G. = $\text{P6}_3/\text{mmc}$, $a = 2.73 \pm 0.02$, $c = 4.44 \pm 0.04$ Å) were reported by Bramman *et al.*^{1,8} A σ -phase in the ternary Mo-Ru-Pd system was reported to exist in a very narrow range. Mo_5Ru_3 or $\text{Mo}_{0.63}\text{Ru}_{0.37}$ is one of the known compositions with tetragonal symmetry (S.G. = $\text{P4}_2/\text{mnm}$, $a = 9.565$ and $c = 4.936$ Å).⁹ However, the physical properties of this σ -phase have not yet been reported. A β -phase in the

ternary Mo-Ru-Pd system has a body-centered cubic structure, which is isostructural with Mo (S.G. = $\text{Im}3\text{m}$, $a = 3.1472$ Å).¹⁰ Vapor pressures, chemical activities and activity coefficients of the Mo-Ru-Pd alloys were determined by Matsui and Naito, since these properties are important factors in the recovery and separation processing of spent nuclear fuel.³ However, no spectroscopic and electromagnetic properties on the ternary alloys have been reported in detail since they were first discovered in the 1960's.

In our previous report, X-ray photoelectron spectroscopic analyses of the quaternary alloys of Mo-Ru-Rh-Pd with a hcp structure were carried out to investigate the chemical states of the constituent elements in the alloys. The core level binding energy of Pd 3d_{5/2} and 3d_{3/2} increased by 0.5-0.9 eV for the quaternary alloys with a hcp structure (ϵ -phase), even though Pauling's electronegativity of Pd is greater than that for Mo. This increase was due to a final state effect, a kind of charge redistribution when chemical bonding occurs between Pd and Mo.¹¹ Furthermore, we observed no discernable shift of Ru 3d and Rh 3d binding energies in the quaternary alloys. We also reported the results of the magnetic susceptibility measurements of the quaternary alloys, $\text{Mo}_{40}\text{Ru}_{40}\text{Rh}_{10}\text{Pd}_{10}$, and $\text{Mo}_{50}\text{Ru}_{20}\text{Rh}_{15}\text{Pd}_{15}$, in which evidence of superconducting transition was observed at 3 and 5 K, respectively.¹² When the elemental Mo content was less than $\sim 30\%$ in the ϵ -phase region of Mo-Ru-Rh-Pd, no superconducting transition was observed above 2 K. However, the superconducting transition was not studied in detail over the different structural regions.

In the present work, we extend our superconductivity studies in novel metal-containing alloys to the ternary Mo-Ru-Pd system and discuss the relationship between superconducting properties and their crystal structures. We prepared several ternary and binary alloys with ϵ , σ and β structure and measured the superconducting transition temperatures (T_c) at low temperatures. The results of the scanning electron micro-

scopic analysis and energy-dispersive x-ray analysis are also reported here.

Experimental Section

The ternary and binary alloys were prepared using an Ar arc melting furnace (Ace Vacuum, Korea). The stoichiometric powdered mixture of Mo (Aldrich, 99.95%), Ru (Aldrich, 99.9%) and Pd (Aldrich, 99.9+%) was pelletized and melted completely three times by turning it upside down in the arc furnace.

An electron probe microanalyzer (EPMA, JEOL JXA-8600) was used to study the microstructure and composition of the alloys. Scanning electron microscopic (SEM) images of the top surface of alloy buttons were obtained. The energy dispersive x-ray (EDX) spectra were analyzed to determine the composition of the alloy.

The powder x-ray diffraction (Siemens D5000) patterns were recorded in the 2θ range of $15-90^\circ$ with an internal standard Pt. The platinum wire on the alloy was pressed flat together in a hydraulic press. The unit cell parameters of the alloys were obtained by least squares refinements of the powder x-ray diffraction (XRD) data.

The magnetic susceptibility of the alloys was measured with an applied magnetic field of 1000 G in the temperature range of 2-300 K using a SQUID magnetometer (Quantum Design). A 70-150 mg pellet of the alloy was used for the measurements. Both zero-field cooled and field cooled measurements were carried out to test the superconducting transitions at low temperatures.

Results and Discussion

The chemical properties of Tc and Ru are considered to be similar, since both Tc and Ru possess the same hcp structure and are completely miscible. This is true for both Rh and Pd and they have the same face-centered cubic (fcc) structure. The ternary Mo-Ru-Pd alloy system, therefore, was used instead of the Mo-Tc-Ru-Rh-Pd alloy in this study.

The ternary alloys of Mo-Ru-Pd (40:30:30, 40:40:20, 40:50:10, 50:20:30, 50:40:10, 57:38:5, 61:37:2) and the binary alloys of Mo-Ru (50:50, 56:44, 62.5:37.5, 90:10) and Mo-Pd (75:25, 50:50, 60:40) were prepared successfully using an Ar arc melting furnace. The EDX analyses on several locations on the quaternary alloys resulted in compositions similar to the charged amount within an experimental error 6-10%. (Table 1) Most of the elemental content of Mo, Ru and Pd matched well with the charged amount. The determination of the exact composition of the products using wet methods was not performed again, since almost the same results were more or less obtained with EDX and ICP-AES composition analyses of the quaternary alloys Mo-Ru-Rh-Pd in the previous studies.¹¹

The powder XRD measurements of the ternary and binary alloys also indicated the successful preparation of the hexagonal close packed ϵ -phase, σ -phase and β -phase in the phase diagram of Mo-Ru-Pd at 1700 °C. (Figure 1) The

Table 1. Compositions of the ternary and binary alloys from the analyses of Energy Dispersive X-ray spectra

No.	Composition	Mo (%)	Ru (%)	Pd (%)
1	Mo ₄₀ Ru ₃₀ Pd ₃₀	43.6	23.2	33.2
2	Mo ₄₀ Ru ₄₀ Pd ₂₀	41.9	39	19.1
3	Mo ₄₀ Ru ₅₀ Pd ₁₀	41.5	47.3	11.2
4	Mo ₅₀ Ru ₂₀ Pd ₃₀	52.4	21.0	26.6
5	Mo ₅₀ Ru ₄₀ Pd ₁₀	50.3	39.9	9.8
6	Mo ₅₇ Ru ₃₈ Pd ₅	55.3	40.0	4.7
7	Mo ₆₁ Ru ₃₇ Pd ₂	59.1	37.4	3.5
8	Mo ₅₀ Ru ₅₀	48.1	51.9	-
9	Mo ₅₆ Ru ₄₄	59.0	41.0	-
10	Mo _{62.5} Ru _{37.5}	62.2	37.8	-
11	Mo ₉₀ Ru ₁₀	89.2	10.8	-
12	Mo ₇₅ Pd ₂₅	74.4	-	25.6
13	Mo ₅₀ Pd ₅₀	48.8	-	51.2
14	Mo ₆₀ Pd ₄₀	59.6	-	40.4

powder XRD studies of the ϵ -phase were similar to those that resulted from the same hexagonal symmetry in the ϵ -phase, known as spherical white inclusions imbedded in the spent nuclear fuels from types such as Pressurized Water Reactors (PWR) and Fast Breeder Reactors (FBR).^{13,14} All the peaks in the powder XRD patterns of Mo₄₀Ru₄₀Pd₂₀, Mo₄₀Ru₃₀Pd₃₀ and Mo₄₀Ru₅₀Pd₁₀ were successfully indexed based on the previously reported XRD data (S.G. = P6₃/mmc, $a = \sim 2.76$ Å, $c = \sim 4.44$ Å). (Figure 1a) As the Ru content increased in Mo-Ru-Pd from 30 to 50%, the unit cell parameters a and c decreased from 2.766 to 2.757 Å and from 4.448 to 4.427 Å, respectively. On the other hand, as the Mo content in the Mo-Ru-Pd increased, the unit cell parameters a and c increased as in the quaternary alloys Mo-Ru-Rh-Pd. These results were consistent with that of the quaternary alloys, Mo-Ru-Rh-Pd with an hcp structure.

For the σ -phase, we found that the tetragonal σ -phase was mostly formed, but usually accompanied with a minor phase of the hexagonal ϵ -phase. A peak at 42.8° was typical of the overlapped peak of (212) and (411) diffractions of the σ -phase and the strongest (101) diffraction of the ϵ -phase. The least squares refinements were tried for the determination of the unit cell parameters of Mo_{62.5}Ru_{37.5} based on the space group, P4₃/mm, which resulted in the unit parameters $a = 9.560(4)$ Å and $c = 4.901(5)$ Å. The determined c value was somewhat smaller than the previously reported value, $c = 4.936$ Å. However, an arrowed peak at 40.5° was not indexable. It seemed to be due to an unidentified phase.

For the β -phase, all the peaks were very well indexed based on the body-centered cubic symmetry (S.G. = Im3m). (Figure 1c) As some of the Mo was replaced by smaller Ru in the β -phase region, all the peaks were shifted to larger 2θ regions. The a unit cell parameter of Mo₉₀Ru₁₀ decreased to 3.1365(4) Å from 3.1472 Å of pure Mo.

For the mixed phase of ϵ and σ (for example, Mo₅₀Ru₂₀Pd₃₀ in Figure 1d), a major phase was definitely the ϵ -phase. It was hard to find strong diffraction peaks from the σ -phase structure, though SEM images of the mixed phase were dif-

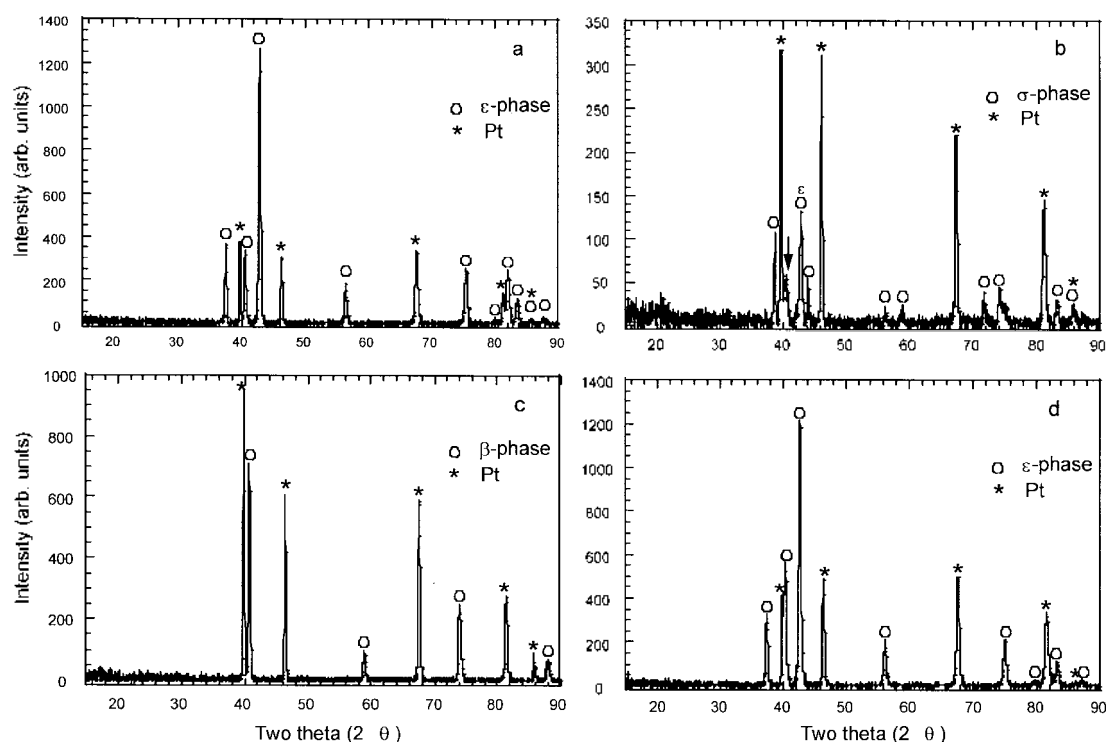


Figure 1. Powder X-ray diffraction patterns of ternary and binary alloys in Mo-Ru-Pd. a. ϵ -phase (40:30:30); b. σ -phase (62.5:37.5:0); c. β -phase (90:10:0); d. ϵ and σ -phase mixture (50:20:30)

Table 2. Unit cell parameters of ternary and binary alloys in Mo-Ru-Pd

No.	Composition	Space group	a (Å)	c (Å)	V (Å ³)	Remark
1	Mo ₄₀ Ru ₃₀ Pd ₃₀	P6 ₃ /mmc	2.766(1)	4.448(2)	29.47(1)	ϵ
2	Mo ₄₀ Ru ₄₀ Pd ₂₀	P6 ₃ /mmc	2.761(1)	4.429(3)	29.23(3)	ϵ
3	Mo ₄₀ Ru ₅₀ Pd ₁₀	P6 ₃ /mmc	2.757(1)	4.427(2)	29.15(2)	ϵ
10	Mo _{62.5} Ru _{37.5}	P4 ₃ /mnm	9.560(4)	4.901(5)	447.9(4)	σ
11	Mo ₉₀ Ru ₁₀	Im3m	3.1365(4)		30.86(1)	β

ferent from those of the ϵ and ϵ -phases.

The unit cell parameters *a* and *c* of the ϵ , σ and β phases were obtained by the least squares refinements based on the previously determined space groups. (Table 2)

Scanning electron microscopy (SEM) measurements on the surface of the alloys showed different surface microstructures, depending on the composition and structure type. (Figure 2) The surface structure of alloys has been known to be closely related to their crystallographic structure and the synthetic condition. In this case, the surface morphology of the top surface seems to be directly related to the crystallographic structure. For the hcp ϵ -phase region in the phase diagram of Mo-Ru-Pd, all the ternary alloys with the hcp structure showed similar surface morphology, that is, rows of round protrusions. There were also lots of voids developed upon crystallization during cooling. (Figure 2a and 2b for Mo₄₀Ru₄₀Pd₂₀ and Mo₄₀Ru₃₀Pd₃₀) The $\sigma + \epsilon$ region looked like a sunflower. (Figure 2c and 3d for Mo₅₀Ru₂₀Pd₃₀ and Mo₅₀Ru₄₀Pd₁₀) The change in surface morphology of the

ϵ -phase seemed to vary with small changes in amount of the σ -phase in the alloy. SEM images of the ϵ and $\sigma + \epsilon$ regions were rather close to each other, indicating complete miscibility between the hexagonal ϵ -phase and the intermediate mixed phase of the $\sigma + \epsilon$. On the other hand, the σ -phase did not show any big void or protrusion, but only a relatively smoother surface with a shallow pattern. (Figure 2e for Mo_{62.5}Ru_{37.5}) This surface pattern was unique to the σ -phase. The β -phase showed quite a different surface morphology from the ϵ -phase and σ -phase. It showed a row of long ridge in part. These different patterns observed on the top surface of the alloy indicated the different structures, respectively. However, special patterns or voids were not observed on the side surface of the alloy buttons.

Single crystal growing experiments have been carried out several times, using CaCl₂ flux. However, they failed to grow single crystals of the ternary alloys (Mo-Ru-Pd), except Mo single crystals. In fact, it was difficult to obtain single crystals of the alloys, using an Ar arc melting furnace. The powder XRD data of the alloys could not be applied to Rietveld analysis to get an atomic position parameter (fractional coordinate) due to their broad peak shapes.

The results of the magnetic susceptibility measurements of the ternary and binary alloys in Mo-Ru-Pd showed evidence of a superconducting transition at 3-9.2 K (Figure 3 and 4). Among the ternary and binary alloys, the σ -phase showed a strong diamagnetism below the superconducting transition. (Figure 3) The σ -phase also showed a sharper transition than the ϵ - and β -phases. The mixed $\sigma + \epsilon$ phase showed a medium diamagnetism and a relatively sharper transition.

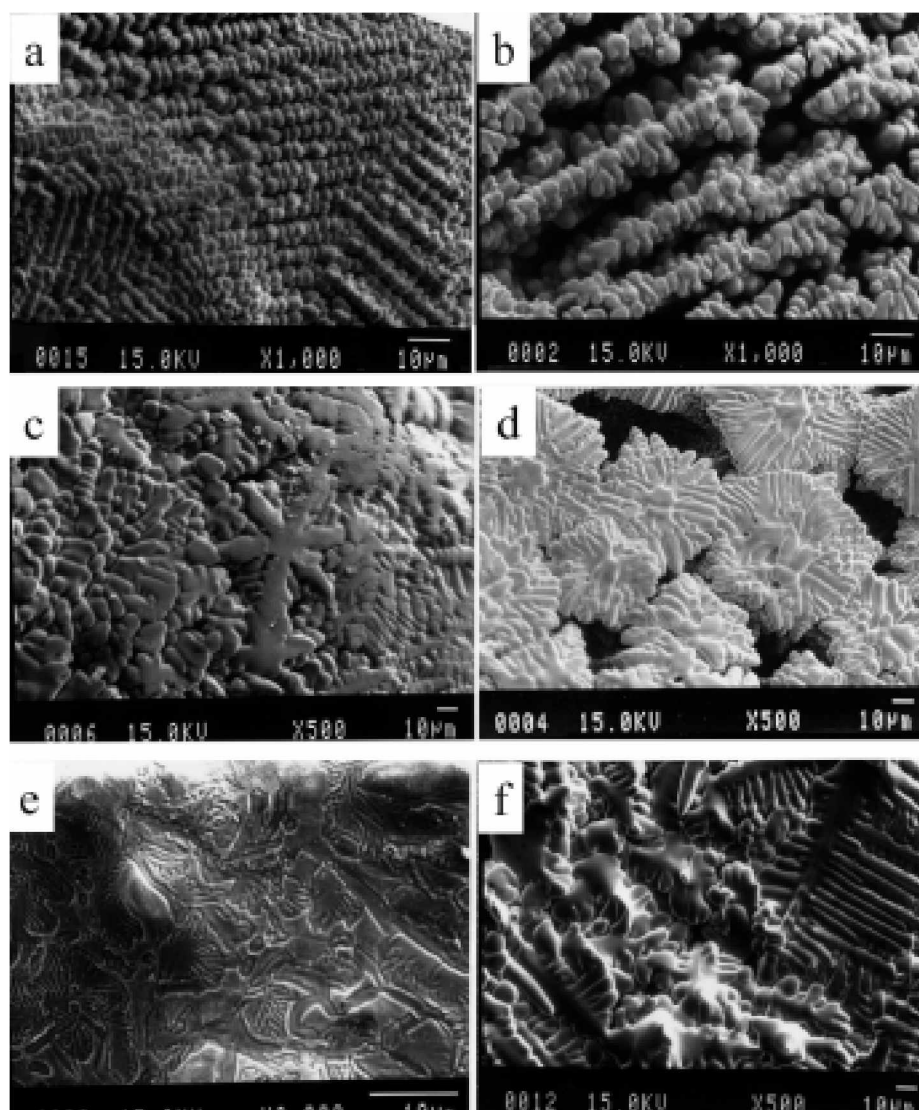


Figure 2. SEM images of the top surface of ternary and binary alloys in Mo-Ru-Pd. a and b are ϵ -phases, c and d are a mixture of the ϵ - and σ -phases, e is the σ -phase and f is the β -phase. (a. 40:40:20; b. 40:30:30; c. 50:20:30; d. 50:40:10; e. 62.5:37.5:0; f. 90:10:0)

These results indicate that the σ -phase is the phase most responsible for the superconducting transition in this phase region near the σ -phase. The formation and uniqueness of σ -phase were indeed confirmed by powder XRD and SEM images of the surface morphology.

Most of the ternary and binary compositions in the σ , ϵ , $\sigma + \epsilon$, $\beta + \sigma + \epsilon$, $\beta + \epsilon$, β , and L+ ϵ phase regions also showed evidence of a superconducting transition. (Figure 4) However, some compositions in the ϵ phase region did not show any evidence of a superconducting transition when the elemental Mo content was less than $\sim 30\%$. (In Figure 4, asterisk marks denote the absence of a superconducting transition above 2K) The absence of superconductivity in the ϵ -phase region when the Mo content was less than $\sim 30\%$ was consistent with the results of superconductivity measurements in the quaternary alloys, Mo-Ru-Rh-Pd.¹²

Among the Mo-rich region ($> 40\%$) in the phase diagram of Mo-Ru-Pd, the highest superconducting transition temperatures were, interestingly, observed in the σ -phase region.

The σ -phase ($\text{Mo}_{62.5}\text{Ru}_{37.5}$ and $\text{Mo}_{50}\text{Ru}_{37}\text{Pd}_2$) showed the highest superconducting transition temperature ~ 9.2 K. This is an interesting and newly discovered result, since a lot of effort has been devoted to investigating the superconducting properties of the many Mo-containing alloys.¹⁵ At this moment, we do not understand the reason why the highest T_c is observed in and near this σ -phase region, since no single crystal X-ray diffraction data have been reported. Different from the superconducting σ -phase, a superconducting transition temperature (~ 9.2 K) was also observed in $\text{Mo}_{50}\text{Ru}_{50}$, which was comparable to the reported values 9.5-10.5 K.^{15,16} The $\text{Mo}_{50}\text{Ru}_{50}$ phase has been reported as a mixed phase of σ and ϵ . It is also noteworthy to compare the superconducting transition temperature of the ternary $\text{Mo}_{40}\text{Ru}_{40}\text{Pd}_{20}$ and $\text{Mo}_{50}\text{Ru}_{20}\text{Pd}_{30}$ with those of quaternary $\text{Mo}_{40}\text{Ru}_{40}\text{Rh}_{10}\text{Pd}_{10}$ and $\text{Mo}_{50}\text{Ru}_{20}\text{Rh}_{15}\text{Pd}_{15}$. Both ternary and quaternary alloys showed similar superconducting transition temperatures at 3-3.7 K and 5-5.8 K, indicating that the amount of Rh did not play an important role. A further confirmation on the

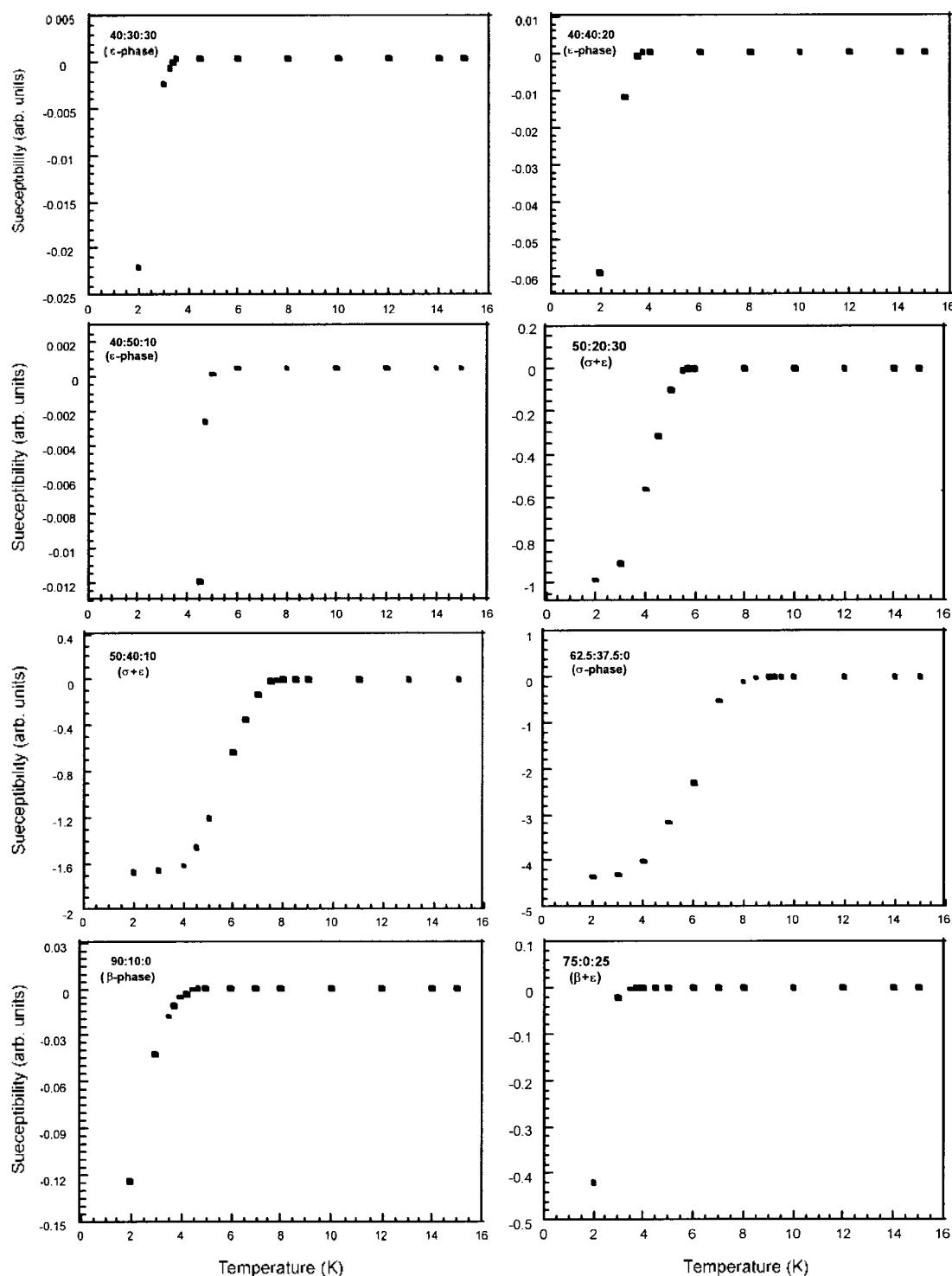


Figure 3. Magnetic susceptibilities of ternary and binary alloys in Mo-Pu-Pd, showing superconducting transitions at 4-9.2 K.

superconducting transition in these phases should be followed by electrical resistivity measurements at low temperatures. Above the superconducting transition temperatures, all the alloys showed a typical Pauli-paramagnetic behavior.

Conclusion

Several superconducting ternary and binary alloys of Mo-

Ru-Pd were prepared using an Ar arc melting furnace. A σ -phase ($\text{Mo}_{62.5}\text{Ru}_{37.5}$ and $\text{Mo}_{61}\text{Ru}_{37}\text{Pd}_2$) as well as $\text{Mo}_{50}\text{Ru}_{50}$ showed the highest superconducting transition temperatures at 9-9.2 K. When the elemental Mo content was less than ~30% in the σ -phase region, there was no superconducting transition observed above 2 K, which was similar to those of the quaternary alloys Mo-Ru-Rh-Pd. Most of the other binary and ternary compositions showed superconducting

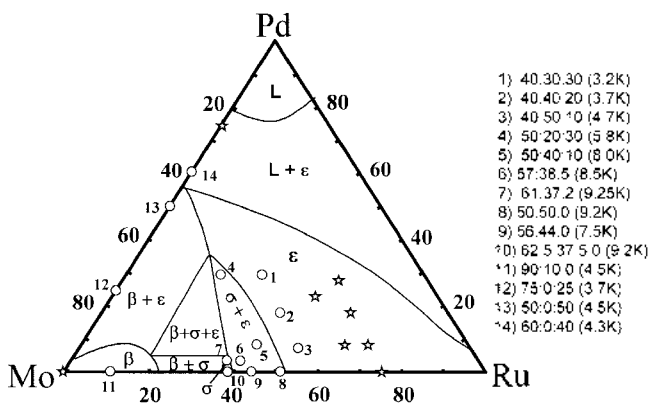


Figure 4. Superconducting composition in the phase diagram of ternary and binary alloy (Mo-Ru-Pd), 1700 °C. The asterisk marks denote the absence of superconductivity above 2 K.

transitions at 3-8.5 K. Measurements of the SEM images of the top surface of the alloy buttons confirmed that the surface morphologies were very closely related to structure type, as well as the composition in these ternary alloy systems. Above the transition temperature, they showed a typical Pauli-paramagnetic behavior.

Acknowledgment. This project has been carried out under the Nuclear R&D program by the Korean Ministry of Science and Technology. We also thank Mr. Kyu-Won Lee for the magnetic susceptibility measurements and Mr. Soon-Dal Park for the electron probe microanalyses.

References

1. Bramman, J. I.; Sharpe, R. M.; Thom, D.; Yates, G. J.

- Nucl. Mater.* **1968**, *25*, 201.
2. Kleykamp, H.; Paschoal, J. O.; Pejsa, R.; Thommler, F. *Journal of Nuclear Materials* **1985**, *130*, 426.
3. Matsui, T.; Naito, K. *Thermochimica Acta* **1989**, *139*, 299.
4. Kleikamp, H. "Constitution and Thermodynamics of the Mo-Ru, Mo-Pd, Ru-Pd and Mo-Ru-Pd Systems", *J. Nucl. Mater.* **1989**, *167*, 49.
5. Matsui, T.; Ohkawa, M.; Sasaki, R.; Naito, K. *J. Nucl. Mater.* **1993**, *200*, 11.
6. Adachi, T.; Ohnuki, M.; Yoshida, N.; Sonobe, T.; Kawamura, W.; Takeishi, H.; Gunji, K.; Kimura, T.; Suzuki, T.; Nakahara, Y.; Muromura, T.; Kobayashi, Y.; Okashita, H.; Yamamoto, T. *J. Nucl. Mater.* **1990**, *174*, 60.
7. Naito, K.; Matsui, T.; Tanaka, Y. *J. Nucl. Sci. Tech.* **1986**, *23*(6), 540.
8. *Pearson's Handbook of Crystallographic Data for Intermetallic Phases*, 2nd Ed.; Villars, P., Calvert, L. D., Eds.; Vol. 4, p 5092.
9. Sigma phase (JC-PDS card number = 39-1086).
10. Beta phase (JC-PDS card number = 42-1120 for Mo).
11. Lee, J.-G.; Park, Y. J.; Kim, J. G.; Pyo, H. Y.; Jee, K. Y.; Kim, W. H.; Jeon, Y. *Journal of Alloys and Compounds* **2000**, *298*, 291.
12. Lee, J.-G.; Park, Y. J.; Kim, J. G.; Jee, K. Y.; Kim, W. H. *Journal of Alloys and Compounds* **1998**, *281*, 264.
13. Kleykamp, H. *Nucl. Technol.* **1988**, *80*, 412.
14. Octavio, J.; Paschoal, A.; Kleikamp, J.; Thummler, F. Z. *Metallkunde* **1983**, *74*, 652.
15. Roberts, B. W. *NBS Technical Note 983, Properties of selected superconductive materials*; 1978 Supplement, 1978.
16. *CRC Handbook of Chemistry and Physics*, 70th Ed.; Weast, R. C. et al., Eds.; E-98 1989-1990.